Structure of fast-ion-conducting lithium and sodium borate glasses by neutron diffraction and reverse Monte Carlo simulations

J. Swenson,* and L. Börjesson
Department of Applied Physics, Chalmers University of Technology, S-412 96 Göteborg, Sweden

W. S. Howells
Rutherford-Appleton Laboratory, Chilton, Didcot, OX11 0QX, United Kingdom
(Received 17 November 1997; revised manuscript received 3 February 1998)

The structures of fast-ion-conducting glasses $(NaZ)_x(Na_2O\text{-}2B_2O_3)_{1-x}$ and $(LiZ)_x(Li_2O\text{-}2B_2O_3)_{1-x}$ ($Z = Cl, Br$) have been examined by neutron diffraction and reverse Monte Carlo (RMC) simulations. The short-range structure of the boron-oxygen network is almost unchanged for increasing dopant salt concentration and independent of the dopant salt, whereas the intermediate range order of the B-O network decreases significantly for increasing dopant salt concentration. The sodium borate glasses are generally slightly more ordered than the corresponding lithium borate glasses. The differences may be explained by the fact that the Li-borate glasses consist of a disordered random mixture of many different types of borate configurations, while the Na-borate glasses are built up by randomly distributed diborate groups, as suggested previously from NMR results. The RMC simulations of the highest LiCl- and NaCl-doped glasses show, however, that large density fluctuations are present within the boron-oxygen network. The voids are of widely different sizes and geometrical shapes. The present findings show that the intermediate-range order of the LiCl- and NaCl-doped glasses is significantly different from that recently reported for the corresponding AgI-doped glass. For the latter the boron-oxygen network forms a more ordered chainlike structure with the salt ions cross linking between the ''chains.'' [S0163-1829(98)00822-4]

I. INTRODUCTION

Glasses with high ionic conductivity presently attract considerable scientific interest because of their potential applications as solid electrolytes in various electrochemical devices such as solid-state batteries, fuel cells, memory devices, chemical sensors, and ''smart windows.'' Furthermore, they are of interest as model materials for investigations of diffusion in disordered systems. In some of the glasses, the diffusion can be extraordinarily fast, comparable to that in liquid electrolytes, and occurs in an otherwise completely frozen environment. Both for technical and fundamental reasons it is of interest to try to understand the fast-ion diffusion on the basis of the microscopic properties. However, despite considerable experimental and theoretical efforts, the conducting mechanism is not yet fully understood.[1] This is partly due to an incomplete knowledge of the microscopic structure, especially on the intermediate length scale, i.e., 4–20 Å, where correlations between various structural subunits may be important.

A particularly interesting class of fast-ion conductors is the metal-halide-doped oxide glasses. The best conducting glasses may reach conductivities up to 10^{-2} S/cm at room temperature.[2] Various spectroscopic techniques have indicated that the introduced dopant ions occupy interstices of the glassy structure without seriously affecting the local structure of the host glass network.[3–6]

Several models, such as the weak electrolyte model,[7–9] the random site model,[10] the dynamic structure model,[11–13] the diffusion pathway model,[4,14,15] the cluster model,[16–22] and the cluster-bypass model,[23] have been proposed to explain the high ionic conductivity, and most of them involve specific or indirect assumptions about the structure of the glass, in particular the cation environment. Given the various assumptions of the different models, it is of interest to seek a better understanding of the structure of the fast-ion-conducting glasses. In some previous papers we have investigated the structures of some of the highest conducting glasses, e.g., AgI-doped borate, phosphate, molybdate, and tungstate glasses, using a combination of diffraction experiments and reverse Monte Carlo modeling.[24–26] For these glasses, considerable intermediate-range ordering was evident from the presence of a sharp diffraction peak at low Q, which grows with increasing AgI content. For the network forming borate and phosphate glasses, the ordering is predominantly due to density fluctuations within the BO or PO network and in none of the molecular and network glasses correlations between the silver and iodine ions contribute substantially to the first (sharp) diffraction peak (FSDP) in the total structure factor. The silver ions were found to coordinate to both oxygens and iodine ions and for the network glasses, the Ag^+ and I^- ions were located in clearly pronounced pathways within the glass network.

The AgI-doped glasses can be regarded as model materials for investigations of the conduction mechanism in amorphous ionic conductors because of their high conductivity. However, it is the lithium- and sodium-containing glasses that seem to be the most suitable materials for technological applications due to the much cheaper price and the higher cell voltages in battery applications. Therefore, we have undertaken a systematic structural study of lithium and sodium-halide-doped borate glasses. The aim is to contribute to an understanding of the microscopic structure and its relation to the ionic conductivity. In particular, we would like to find a

structural explanation for why the lithium and sodium borate glasses have lower conductivities than the corresponding silver borate glasses and hence, to discriminate structural features that are important for high ionic conductivity. Such knowledge may be useful for optimizing amorphous ionic conductors for future applications.

We have chosen to study metal-halide-doped borate glasses, because they have relatively high ionic conductivities, wide glass-forming composition range, are chemical stable, and readily form glasses. In this paper, we report on structural investigations of $(MZ)_x(M_2O\text{-}2B_2O_3)_{1-x}$ glasses ($x=0-0.6$), where $M=$Li,Na and $Z=$Cl or Br, by using neutron diffraction. In view of the assumptions of the structural models above it is of particular interest to get a better understanding of how the dopant ions are introduced. We have therefore used the method of isotopic variation of Li and Cl to get a better determination of the local structure around these ions. We have also performed reverse Monte Carlo (RMC) (Refs. 27 and 28) simulations of the glasses $M_2O\text{-}2B_2O_3$ and MCl-$M_2O\text{-}2B_2O_3$ ($M=$Li,Na) in order to investigate changes in the intermediate-range structure since they appear to play an important role in several models. The results will be compared with various structural models proposed for ion-conducting glasses and will also as mentioned be compared with recent results for AgI-doped glasses.[24–26]

II. EXPERIMENTAL DETAILS

Glasses of compositions $(LiCl)_x\text{-}(Li_2O\text{-}2B_2O_3)_{1-x}$ ($x=0-0.6$), LiBr-$Li_2O\text{-}2B_2O_3$, and $(NaZ)_x(Na_2O\text{-}2B_2O_3)_{1-x}$ ($x=0$,0.5 and $Z=$Cl,Br) were prepared using melt quenching according to procedures described previously.[29,30] For the LiCl-$Li_2O\text{-}2B_2O_3$ composition two additional samples were prepared, one with an appropriate combination of ^{6}Li and ^{7}Li to give zero neutron scattering length of Li and one where chlorine was isotopically enriched in ^{37}Cl. In all samples boron was isotopically enriched in ^{11}B (99%) in order to minimize the influence of the high neutron absorption of ^{10}B present in natural boron. The samples, which were in shapes of cylindrical rod with a diameter of 9 mm and a length of 50 mm, were mounted in thin-walled vanadium containers. The neutron diffraction experiments were performed on the time-of-flight Liquid and Amorphous Materials Diffractometer at the pulsed neutron source ISIS, Rutherford Appleton Laboratory, UK. The diffractometer has been described in detail elsewhere.[31] Time-of-flight spectra were recorded separately for each group of detectors at the angles 150°, 90°, 58°, 35°, 20°, 10°, and 5° and also for monitors in the incident and transmitted beam, respectively.

The data of each detector group were corrected separately for background and container scattering, absorption, multiple scattering, and inelasticity effects and normalized against the scattering of a vanadium rod to obtain the structure factor $S(Q)$, following the procedure described in Ref. 32. The absorption corrections required some caution because of the high absorption cross section (about 3×10^{-23} cm^2 for a neutron wavelength of 1.8 Å). It was carefully checked in the same manner as for the binary borates described in Ref. 33. The corrected individual data sets obtained at each angle were then combined to obtain a wide Q range and to improve the statistics. For each data set we only used the Q range that agreed with other data sets in the overlapping Q region.

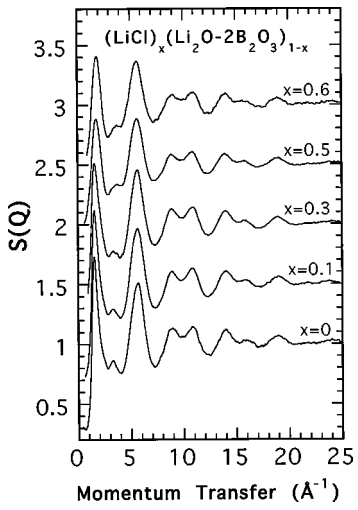

FIG. 1. Structure factors $S(Q)$ of $(LiCl)_x(Li_2O\text{-}2B_2O_3)_{1-x}$ ($x=0-0.6$). The upper curves have been shifted vertically for clarity.

The obtained structure factor $S(Q)$ of each sample was Fourier transformed to obtain the total neutron weighted pair-correlation function

$$G(r)=\frac{\sum_{i=1}^{n} c_i b_i^2}{2\pi^2\rho^0\left(\sum_{i=1}^{N} c_i b_i\right)^2}\int_0^\infty Q[S(Q)-1]\sin(Qr)\,dQ+1, \tag{1}$$

where ρ^0 is the average number density, and c_i and b_i are the concentration and neutron-scattering length of atom i, respectively. The total $G(r)$ can be expressed as a neutron weighted (i.e., dependent upon the scattering lengths of the constituent atoms) sum of the partial pair-correlation functions $g_{ij}(r)$ according to

$$G(r)=\frac{\sum_{i,j=1}^{n} c_i c_j\langle b_i\rangle\langle b_j\rangle g_{ij}(r)}{\left(\sum_{i=1}^{n} c_i b_i\right)^2}. \tag{2}$$

Before the Fourier transformations were done the structure factors were truncated at $Q_{\max}=30$ Å^{-1} in order to avoid small systematic errors of the high-Q data. Termination ripples in the correlation function caused by the Fourier transformation and this truncation were reduced by multiplying the integrand in Eq. (1) with the Lorch modification function,[34] although this is at the expense of a somewhat reduced real-space resolution.

III. EXPERIMENTAL RESULTS

A. Lithium borate glasses

The structure factors $S(Q)$ of the investigated fast-ion-conducting glasses are shown in Figs. 1–3. Some of the results have appeared in previous preliminary reports.[5,6] Figure 1 shows the structure factors of the glass system

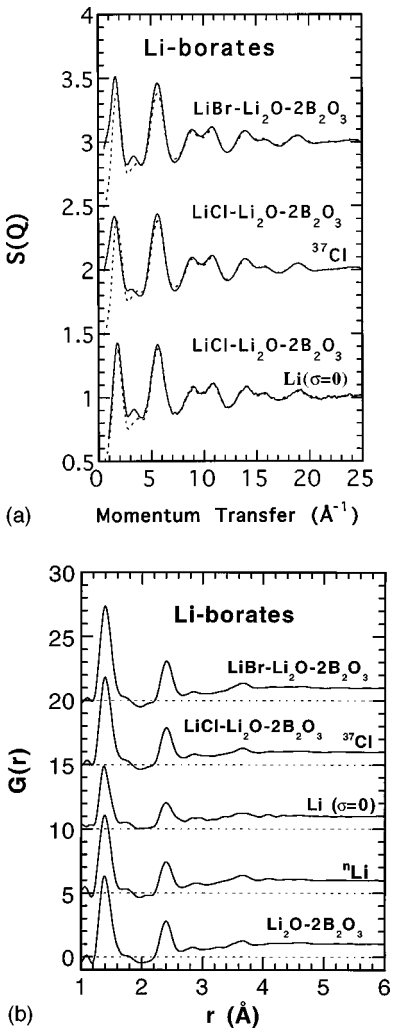

FIG. 2. (a) Structure factors $S(Q)$ of LiBr-Li_2O-$2B_2O_3$ and LiCl-Li_2O-$2B_2O_3$, one with a mixture of ^{6}Li and ^{7}Li to give zero scattering length of Li and one with ^{37}Cl enriched chlorine. The structure factors have been compared with $S(Q)$ of LiCl-Li_2O-$2B_2O_3$ containing natural Li and Cl (dashed lines). (b) shows the pair-correlation functions $G(r)$ of Li_2O-$2B_2O_3$ and the same glasses as were shown in (a). The upper curves have been shifted vertically for clarity.

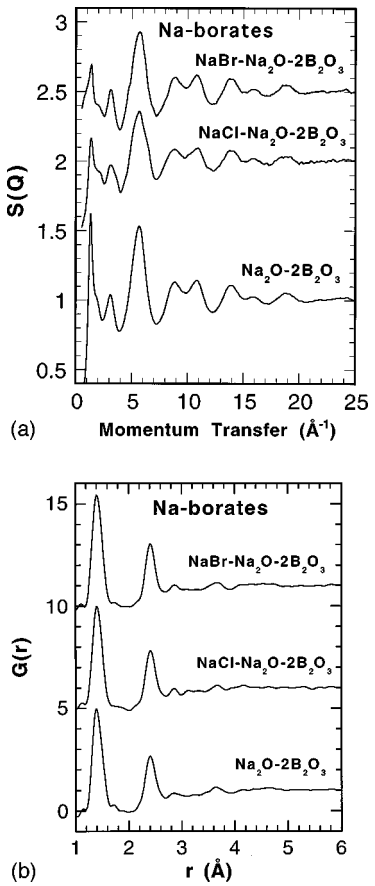

FIG. 3. (a) Structure factors $S(Q)$ and (b) pair-correlation functions $G(r)$ of $(NaCl)_x(Na_2O\text{-}2B_2O_3)_{1-x}$ $(x=0,0.5)$ and NaBr-Na_2O-$2B_2O_3$. The upper curves have been shifted vertically for clarity.

$(LiCl)_x(Li_2O\text{-}2B_2O_3)_{1-x}$ $(x=0-0.6)$. It is there evident that all glasses show almost identical results for the high-Q range, indicating very similar short-range structures, and only small differences in the low-Q region. It is worth noticing that the predominant part (about 60% or more) of the scattering of the present glasses is from the B-O network. The insensitivity of the high-Q range to metal-halide doping supports previous Raman and neutron diffraction results,[4–6] which indicate that the halide salt does not affect the short-range order of the host boron-oxygen network. In the low-Q region, the FSDP broadens and shifts continuously to higher Q values with increasing dopant salt concentration x. For $x=0$, the peak position is at 1.53 Å^{-1} and for $x=0.6$, the position of the FSDP has shifted to 1.87 Å^{-1}, indicating that density fluctuations occur on shorter length scales. This is interesting because the behavior is completely opposite to that observed for AgI-doped borate glasses,[6,25] for which a new peak appears around 0.8 Å^{-1} and grows with increasing AgI content.

Figure 2(a) shows two structure factors of LiCl-Li_2O-$2B_2O_3$, one with a mixture of ^{6}Li and ^{7}Li to give zero scattering length of Li an one with ^{37}Cl enriched chlorine, and $S(Q)$ of LiBr-Li_2O-$2B_2O_3$. The structure factors have been compared with $S(Q)$ of LiCl-Li_2O-$2B_2O_3$ containing natural Li and Cl (dashed lines). Figure 2(b) shows the atomic pair-correlation functions $G(r)$ for Li_2O-$2B_2O_3$ and the same glasses as were shown in Fig. 2(a). Figure 2(a) shows that the high-Q range is almost unaffected by the changes of cation and anion, indicating that the high-Q-range oscillations are dominated by well-defined distances within the boron-oxygen network (which do not change by the introduction of the dopant salt). This can also be established from the short-range real-space correlations shown in Fig. 2(b), where it is seen that the two first peaks in $G(r)$ occur at the same position and with almost the same width for all the investigated glasses. Thus, the B-O network of all the investigated glasses has a very similar short-range order. The differences are mainly seen on an intermediate length scale in the Q region below 4 Å^{-1}.

The largest change is observed for the ^{37}Cl sample in the lowest Q region, which has a FSDP at a slightly lower Q value and a substantially higher intensity at the low-Q side of the FSDP. However, most differences are relatively small. The small differences between the LiCl- and LiBr-doped glasses indicate that their structures are very similar. There is no obvious particular feature observed in $S(Q)$ that can be

related to the correlations of the introduced salt ions. The most interesting difference between the structure factors shown in Fig. 2(a) is the change of the intensity at Q values below the FSDP for different Li halides. The intensity increases with decreasing scattering length of the anion ($b_{(^{n}\mathrm{Cl})} > b_{(\mathrm{Br})} > b_{(^{37}\mathrm{Cl})}$), indicating that correlations within the B-O network cause high scattering intensity below 1.5 Å^{-1} and that the halides contribute negatively in this range of $S(Q)$. However, we note that no anomalous low-Q peak, similar to that observed for the highly AgI-doped borate glasses,[25] is produced. Rather, it is evident from Fig. 2(a) that the intermediate-range density fluctuations of Li_2O-$2B_2O_3$ decrease drastically with LiCl and LiBr doping.

B. Sodium borate glass

In Figs. 3(a) and 3(b) the structure factors and pair correlation functions, respectively, of Na_2O-$2B_2O_3$ and NaZ-Na_2O-$2B_2O_3$ (Z=Br,Cl) are shown. As for the lithium borate glasses only minor changes in the high-Q range are observed to occur on salt doping [see Fig. 3(a)]. The short-range order of the B-O network is not only almost unaffected of salt doping, it is also similar for lithium and sodium borate glasses. The most obvious difference in $G(r)$ between those glasses [see Figs. 2(b) and 3(b)] is seen for $1.7 < r < 2.5$ Å. This is due to the fact that the nearest Li-O distance at about 2.0 Å is significantly lower than the nearest Na-O distance at about 2.3 Å,[33] and also due to the large difference in scattering length between natural Li (negative scattering length due to the high amount of ^{7}Li and Na (positive scattering length). Correlations between Li and a nucleus with positive scattering lengths result in negative peaks in $G(r)$ [see Eq. (2)]. In the low-Q region, however, there are differences between the lithium and sodium borate glasses [see Figs. 1 and 3(a)]. In the case of the sodium borate glasses, the position of the FSDP is almost unchanged at about 1.35 Å^{-1}; however, its intensity decreases dramatically for both NaCl and NaBr doping. In addition, the NaBr-doped glass shows a weak shoulder at about 0.9 Å^{-1}.The origin of this shoulder is probably similar to the increased intensity below the Q value of the FSDP for the lithium-halide-doped glasses, as discussed above. Considering the length scale of the density fluctuations, the doped Na-borate glasses show an intermediate behavior compared to the LiCl- and AgI-doped borate glasses.

C. Short-range order of LiCl-Li_2O-$2B_2O_3$

In Fig. 4 we show the difference in the pair-correlation function $G(r)$, $\Delta G(r)$, between the Li ($\sigma=0$) and ^{n}Li samples, and between the ^{n}Cl and ^{37}Cl samples, respectively. Before the subtractions were performed, the pair-correlation functions of the three samples were scaled by the area of the first B-O peak, because the relative scattering cross sections of the B-O correlations to the total $G(r)$ are different. In this way, all the intra B-O network correlations are canceled and the difference curves contain only correlations involving Li and Cl, respectively. Let us first consider the Li correlations shown in Fig. 4 (curve a), where $\Delta G(r) = 0.0141 G_{\mathrm{BLi}}(r) + 0.0220 G_{\mathrm{OLi}}(r) - 0.0016 G_{\mathrm{LiLi}}(r) + 0.0052 G_{\mathrm{LiCl}}(r)$. The peak from the nearest Li-O distance

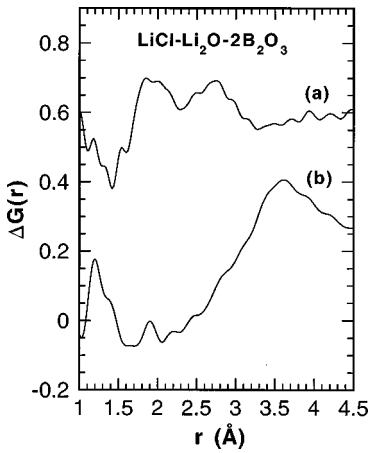

FIG. 4. Difference functions $\Delta G(r)$ obtained from the difference between the following pair-correlation functions $G(r)$ of LiCl-Li_2O-$2B_2O_3$ glasses with different isotope mixtures: (a) one with a mixture of ^{6}Li and ^{7}Li to obtain zero scattering from Li and one with natural Li and (b) the difference between a sample with natural Cl and one where chlorine was isotopically enriched in ^{37}Cl. The first peak (B-O) in the pair-correlation functions is scaled to the same area. Curve (a) has been shifted vertically 0.4 for clarity.

at 2.0 ± 0.1 Å, which gave a negative contribution in Fig. 2, is again evident in the $\Delta G(r)$, but now as a positive contribution because of the subtraction. There is another broad peak at 2.75 ± 0.1 Å, which we attribute to involve predominantly the nearest Li-B and Li-Cl correlations, in accordance with the structure of glassy[33] and crystalline Li_2O-$2B_2O_3$ (Refs. 35 and 36) and crystalline LiCl.[37] Unfortunately, the difference in scattering length between Li ($\sigma=0$) and the ^{n}Li is too small to be able to estimate the nearest Li-Li distance [which should produce a negative peak in $\Delta G(r)$]. The difference curve of ^{n}Cl and ^{37}Cl in Fig. 4 (curve b) is given by $\Delta G(r) = 0.0163 G_{\mathrm{BCl}}(r) + 0.0255 G_{\mathrm{OCl}}(r) - 0.0038 G_{\mathrm{LiCl}}(r) + 0.0037 G_{\mathrm{ClCl}}(r)$. It shows a large broad peak at about 3.6 ± 0.1 Å and essentially no correlations below 2.5 Å. The broad peak probably contains several different nearest interatomic distances (Cl-O, Cl-B, and Cl-Cl), and it is therefore difficult to separate the various correlations involving Cl by this method. However, the broad featureless peak indicates that none of the correlations are particularly well defined.

D. Short-range order of NaCl-Na_2O-$2B_2O_3$

Figure 5 shows the difference in $G(r)$, $\Delta G(r)$, between the glasses NaCl-Na_2O-$2B_2O_3$ and Na_2O-$2B_2O_3$. The individual $G(r)$ are scaled by the area of the first B-O peak. The subtraction is performed with the assumption that the short-range order of the BO network is essentially unaffected of the metal-halide doping. The difference curve

$$\Delta G(r) = 0.0083 G_{\mathrm{BNa}}(r) + 0.0222 G_{\mathrm{BCl}}(r) + 0.0130 G_{\mathrm{ONa}}(r) + 0.0346 G_{\mathrm{OCl}}(r) + 0.0029 G_{\mathrm{NaNa}}(r) + 0.0093 G_{\mathrm{NaCl}}(r) + 0.0041 G_{\mathrm{ClCl}}(r)$$

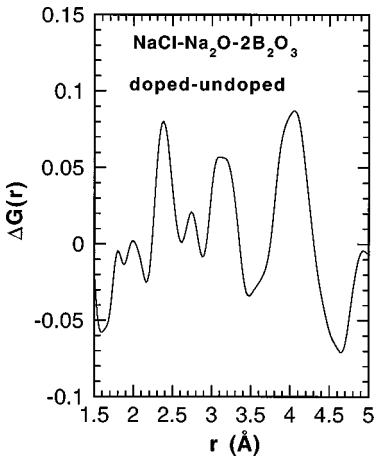

FIG. 5. Difference function $\Delta G(r)$ obtained from the difference between the pair-correlation functions $G(r)$ of the glasses $NaCl\text{-}Na_2O\text{-}2B_2O_3$ and $Na_2O\text{-}2B_2O_3$. The first peak (B-O) in the pair-correlation functions is scaled to the same area.

is not showing any correlations within the BO network if this assumption is validated. Three main peaks can be clearly distinguished in $\Delta G(r)$ located at 2.4 ± 0.1, 3.1 ± 0.1, and 4.0 ± 0.1 Å, respectively. By comparison with data of other similar samples and also with x-ray diffraction results we attribute the first peak to the first Na-O shell,[33,38,39] the second peak to predominantly involve the nearest Na-B and Na-Cl correlations, and the third peak at 4.0 ± 0.1 Å is probably due to many different correlations involving Na and Cl, and perhaps also to differences in the BO-network ordering between the two samples. The small peak located at 2.80 ± 0.1 Å may also be significant, since it coincides with the second Na-O shell in crystalline $Na_2O\text{-}2B_2O_3$ (Ref. 40) and glassy $Na_2O\text{-}2B_2O_3$ (Ref. 39) and also with the nearest Na-Cl distance in crystalline NaCl.[41]

IV. STRUCTURAL MODELING

To obtain further insights into the structures it is desirable to perform some kind of modeling of the glass structures. Molecular dynamics (MD) simulations have already been performed on $(LiCl)_x(Li_2O\text{-}2B_2O_3)_{1-x}$ $(x=0,0.6)$ (Ref. 42) and compared to the neutron data presented here. The MD simulations were able to reproduce the high-Q part of $S(Q)$ relatively well, but large deviations from the experimental data were found in the low-Q region. The probable reason for these deviations is the difficulties to find accurate enough approximations of all the included pair potentials to reproduce both the short- and the intermediate-range order of such chemically complicated systems as the present glasses. We have taken an alternative route to create structural models of the glasses by using the RMC method,[27,28] which makes direct use of the available experimental data without any assumption of the potentials involved. It has recently been successfully applied to other network and fast-ion-conducting glasses.[24,25,28] Here, we will present results from RMC simulations on the glasses $(LiCl)_x(Li_2O\text{-}2B_2O_3)_{1-x}$ and $(NaCl)_x(Na_2O\text{-}2B_2O_3)_{1-x}$ $(x=0,0.5)$.

A. The reverse Monte Carlo method

The RMC method is based on the Metropolis Monte Carlo algorithm (Ref. 43) (Markov chain, periodic boundary conditions, etc.), but instead of minimizing the energy, one minimizes the squared difference between the experimental structure factor and the structure factor calculated from the computer configuration. The structure of this computer configuration is modified by moving the atoms randomly until the calculated structure factor agrees with the experimental data within the experimental errors. Moves are only accepted if they are in accordance with certain constraints, e.g., closest atom-atom distances (see below). In this way, the RMC method produces three-dimensional models of disordered materials that agree quantitatively with the available diffraction data (provided that the data do not contain significant systematic errors) and experimental density without using any interatomic potentials. For more details of the RMC technique see Refs. 44 and 45.

B. Simulation procedure

To be able to simulate the intermediate-range structural order the configuration has to be large enough so that the corresponding box size does not influence the ordering in question, i.e., a large number of atoms must be used. The computer configurations of the present undoped $(x=0)$ and doped $(x=0.5)$ glasses contained 3900 and 3600 atoms, respectively. The cubic box lengths were given values corresponding to the experimentally measured densities, i.e., 33.39 and 34.50 Å for the undoped lithium and sodium borate glasses, respectively, and 34.13 and 35.57 Å for the LiCl- and NaCl-doped glasses, respectively. Periodic boundary conditions were used.

In order to ensure physically realistic configurations, in the sense that there is no overlap of atoms and that the B and O atoms form a properly connected network, we ran hard sphere Monte Carlo simulations with certain constraints applied. This is important since without using constraints it is unlikely that the RMC method will produce physically sensible structural models.[46] RMC tends to produce the most disordered structure that is consistent with the experimental data and the constraints, i.e., the configurational entropy is maximized. However, the number of possibilities to fit the data will be significantly reduced using appropriate constraints and the final structural model is likely to be much more realistic. The constraints we used were of two kinds: closest atom-atom approach and connectivity. The closest distance that two atoms were allowed to approach were determined from the experimental results, e.g., the pair-correlation function. The following closest atom-atom distances were used in the simulations: 1.25 Å for B-O, 1.75 Å for Li-O, 2.1 Å for O-O, 2.2 Å for B-B and Na-O, 2.3 Å for Li-Cl, 2.4 Å for Li-B, Li-Li, and Na-Cl, 2.5 Å for Na-B and Na-Na, 2.6 Å for O-Cl, 2.8 Å for B-Cl, and 3.0 Å for Cl-Cl. the constraints on the B-O-network connectivity were applied on the basis of results obtained from NMR,[47–49] Raman,[50,51] and infrared experiments.[52] These experiments have shown that the addition of M_2O to B_2O_3 causes a progressive increase in the number of four-coordinated borons at the expense of three-coordinated ones. At the composition $M_2O\text{-}2B_2O_3$ the fraction of four-coordinated borons is close

to 45%. Therefore, we have applied the constraints that all the oxygens are coordinated to two borons and that 45% of the borons are coordinated to four oxygens. The remaining borons are coordinated to three oxygens. The B-O distance was allowed to vary from 1.25 to 1.65 Å. In this way we have ensured that BO_3 and BO_4 units are formed and that they are linked together in a network. However, here it should be noted that although the fractions of BO_3 and BO_4 units are the same for the Li and Na-borate glasses there are differences between the glasses in how these units are connected to larger borate configurations. ^{10}B NMR studies of Li_2O-$2B_2O_3$ (Ref. 49) and Na_2O-$2B_2O_3$ (Ref. 53) have shown that the glass network of Li_2O-$2B_2O_3$ consists of the four borate configurations, diborate, tetraborate, metaborate, and loose BO_4^- units, while the glass network of Na_2O-$2B_2O_3$ consists only of diborate groups. Such larger structural groups have, however, not been built in by constraints in the RMC models. After the BO network was formed all the Cl^- and Li^+ or Na^+ ions were randomly introduced into the computer boxes of the glasses. Before the fitting procedure to the experimental data was started the added ions were moved apart from each other and from the B and O atoms in order to fulfill the closest atom-atom constraints.

We have two and three available experimental structure factors of the undoped and doped lithium-containing glasses, respectively. However, we will not use the structure factors of the samples with a mixture of ^{6}Li and ^{7}Li to give zero scattering length of Li. The reason for this is that the high absorption cross section of ^{6}Li makes the absorption correction difficult for the low-Q region of those samples, and the data may, therefore, contain some quantitative systematic errors that are likely to affect the intermediate range order of the structural models.

C. Results

In Figs. 6(a) and 6(b) the structure factors of the RMC-produced models of the lithium and sodium borate glasses, respectively, are compared with those obtained experimentally. Figure 6(a) shows two structure factors of the LiCl-Li_2O-$2B_2O_3$ glass: one for the sample with natural isotopes and one for the sample containing ^{37}Cl. Considering the high absorption cross section of the three samples, the overall structure factors are well reproduced in both simulations, although there are some discrepancies in the low-Q region for the ^{37}Cl sample. The structure factors of the undoped and doped sodium borate glasses, respectively [see Fig. 6(b)], are well reproduced over the whole Q range (0.5–30 Å^{-1}). The configurations should therefore contain essential structural information related to both the short-range order of the BO network and the type of intermediate-range ordering giving rise to the FSDP's.

1. Intermediate-range order

In Figs. 7(a) and 7(b) we plot the partial structure factors $S_{ij}(Q)$ of the RMC-produced configurations of Li_2O-$2B_2O_3$ and Na_2O-$2B_2O_3$, respectively. For Li_2O-$2B_2O_3$ [see Fig. 7(a)] it is evident that all the partial structure factors contribute to the experimentally observed FSDP at 1.53 Å^{-1}, since the dips (''negative peaks'') in $S_{\mathrm{BLi}}(Q)$ and $S_{\mathrm{OLi}}(Q)$ at similar Q values turn positive in total $S(Q)$ due to the negative scattering length of natural lithium. Thus, $S_{\mathrm{BLi}}(Q)$ and $S_{\mathrm{OLi}}(Q)$ contribute to the FSDP in total $S(Q)$ due to the negative scattering length of lithium, although it should be noted that they in reality show an anticorrelation in the actual Q range, in accordance with the shown partial structure factors. The FSDP at 1.35 Å^{-1} of Na_2O-$2B_2O_3$ is entirely due to correlations within the B-O network [see Fig. 7(b)]. The three partial structure factors $S_{\mathrm{BB}}(Q)$, $S_{\mathrm{BO}}(Q)$, and $S_{\mathrm{OO}}(Q)$ all have peaks at about 1.35 Å^{-1}, while the other three partial structure factors show dips at similar Q values. However, it should here be noted that $S_{\mathrm{NaNa}}(Q)$ has a prepeak at a lower Q value (1.0 Å^{-1}) than the FSDP in the total $S(Q)$. The fact that the partial structure factors $S_{\mathrm{BLi}}(Q)$ and $S_{\mathrm{OLi}}(Q)$ for Li_2O-$2B_2O_3$, and $S_{\mathrm{BNa}}(Q)$ and $S_{\mathrm{ONa}}(Q)$ for Na_2O-$2B_2O_3$ show rather well-defined dips at about the same Q values as the partial structure factors of the B-O network have peaks, i.e., the correlations are in antiphase to the correlations within the B-O network, indicates that the cations form bridges between neighboring BO_4^- units. This cross-linking behavior of the cations is even more pronounced for the Ag_2O-$2B_2O_3$ glass.[25] The results are also in support of a

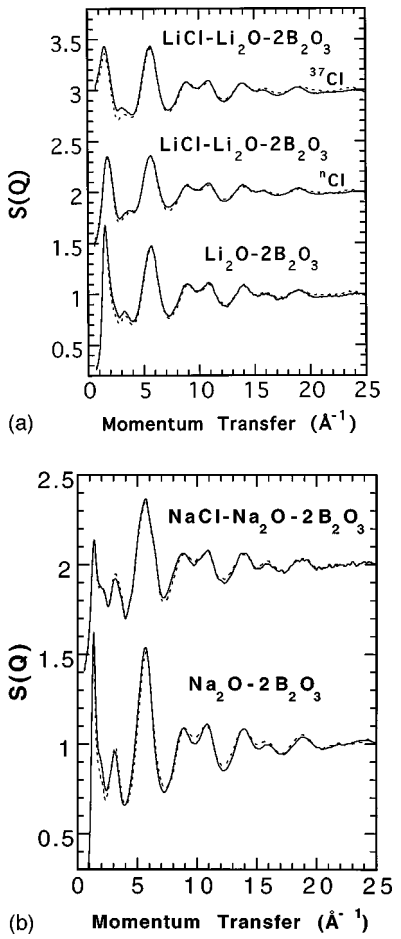

FIG. 6. Experimental structure factors (full lines) and computed neutron weighted total structure factors (dashed lines) for the RMC configurations of (a) Li_2O-$2B_2O_3$ and LiCl-Li_2O-$2B_2O_3$ and (b) Na_2O-$2B_2O_3$ and NaCl-Na_2O-$2B_2O_3$. Two structure factors of LiCl-Li_2O-$2B_2O_3$ are shown, one with natural C and one with ^{37}Cl. The upper curves have been shifted vertically 1.0 for clarity.

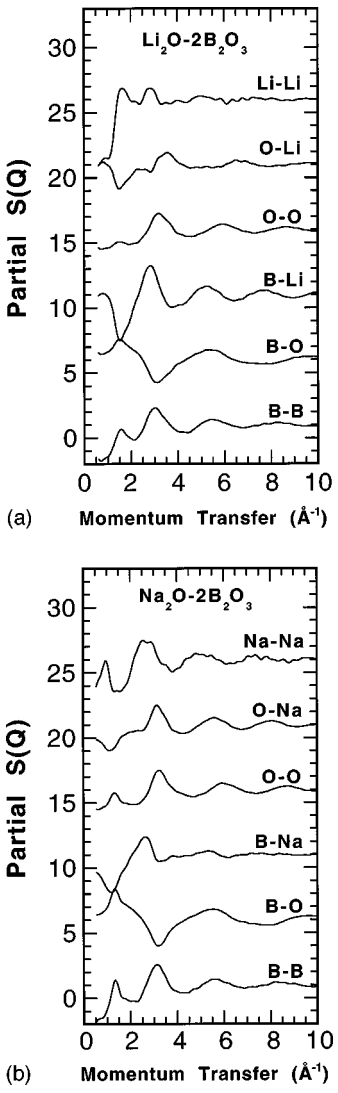

FIG. 7. Partial structure factors $S_{ij}(Q)$ calculated from the RMC configurations of (a) Li_2O-$2B_2O_3$ and (b) Na_2O-$2B_2O_3$. The upper curves have been shifted vertically for clarity.

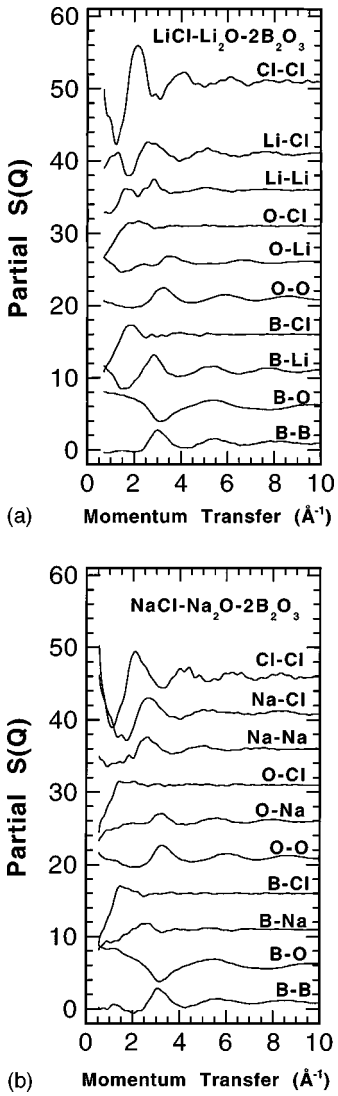

FIG. 8. Partial structure factors $S_{ij}(Q)$ calculated from the RMC configurations of (a) LiCl-Li_2O-$2B_2O_3$ and (b) NaCl-Na_2O-$2B_2O_3$. The upper curves have been shifted vertically for clarity.

proposed void-based model for the intermediate-range structure of network modified glasses.[54–56]

Figures 8(a) and 8(b) show the partial structure factors $S_{ij}(Q)$ of the LiCl- and NaCl-doped glasses, respectively. By comparing the two figures it is evident that the intermediate-range order is relatively similar for the two glasses. The lost (or almost lost in the case of the NaCl-doped glass) prepeaks in the partial structure factors $S_{\mathrm{BB}}(Q)$, $S_{\mathrm{BO}}(Q)$, and $S_{\mathrm{OO}}(Q)$ show that the correlations within the B-O network give no contribution to the FSDP's at 1.8 and 1.35 Å^{-1} in the total $S(Q)$ of the LiCl- and NaCl-doped glasses, respectively. This is not an expected result if one takes into consideration that the introduced dopant salts have caused an expansion of the B-O network with about 35% compared to the undoped glasses. Thus, there must be some kind of voids within the B-O network, which are likely to give rise to a peak at relatively low Q. The explanation of the absence of a prepeak must be that there is no particular characteristic intermediate distance within the B-O network similar to what was found for the AgI-doped glass.[25] Rather, the B-O network of the LiCl- and NaCl-doped glasses must contain voids of widely different sizes and geometrical shapes. For the LiCl-doped glass the results indicate that the origin of the experimentally observed FSDP at $Q_1 \approx 1.8$ Å^{-1} in the total $S(Q)$ is due to a combination of peaks (due to nearest-neighbor distances) in the partial structure factors $S_{\text{Cl-Cl}}(Q)$, $S_{\text{Cl-B}}(Q)$, and $S_{\text{Cl-O}}(Q)$, and dips (''negative peaks'') in the partial structure factors $S_{\text{Li-B}}(Q)$, $S_{\text{Li-O}}(Q)$, and $S_{\text{Li-Cl}}(Q)$. These dips turn positive in the total $S(Q)$ due to the negative scattering length of natural lithium. The FSDP in the total $S(Q)$ of the NaCl-doped glass is not due to any individual peaks in the partial structure factors. Rather, the FSDP is produced by the summation of the partial structure factors, due to the fact that some of them show decreasing intensity towards $Q=0$ while others rise with decreasing Q over the Q region in question. This is also the reason for the sharpness of the experimentally observed FSDP. Thus, the structures of the NaCl- and LiCl-doped glasses show no pronounced intermediate-range order, and are, therefore, much more disordered than the AgI-doped glass with its highly ordered B-O network.[25]

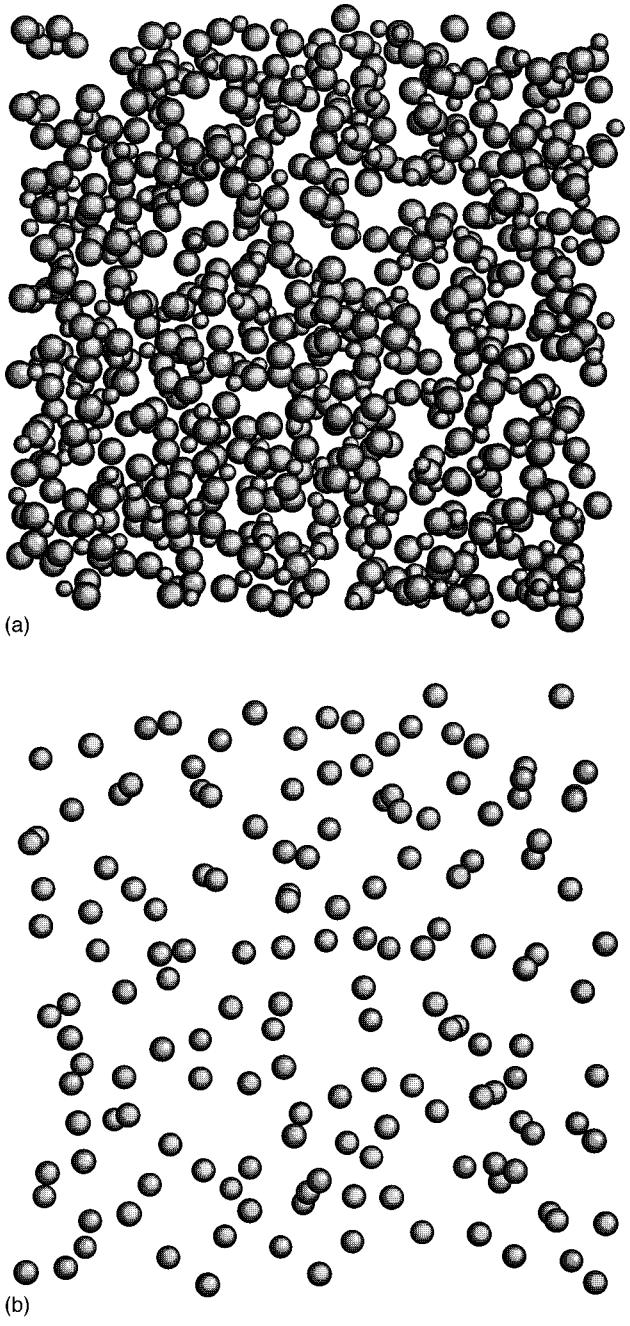

FIG. 9. A 10-Å-thick slice of the RMC configuration of Li_2O-$2B_2O_3$.(a) shows the structure of the B-O network and (b) the distribution of lithium ions. The radii of the chemical components are B=0.5, O=0.8, and Li^+=0.7 Å.

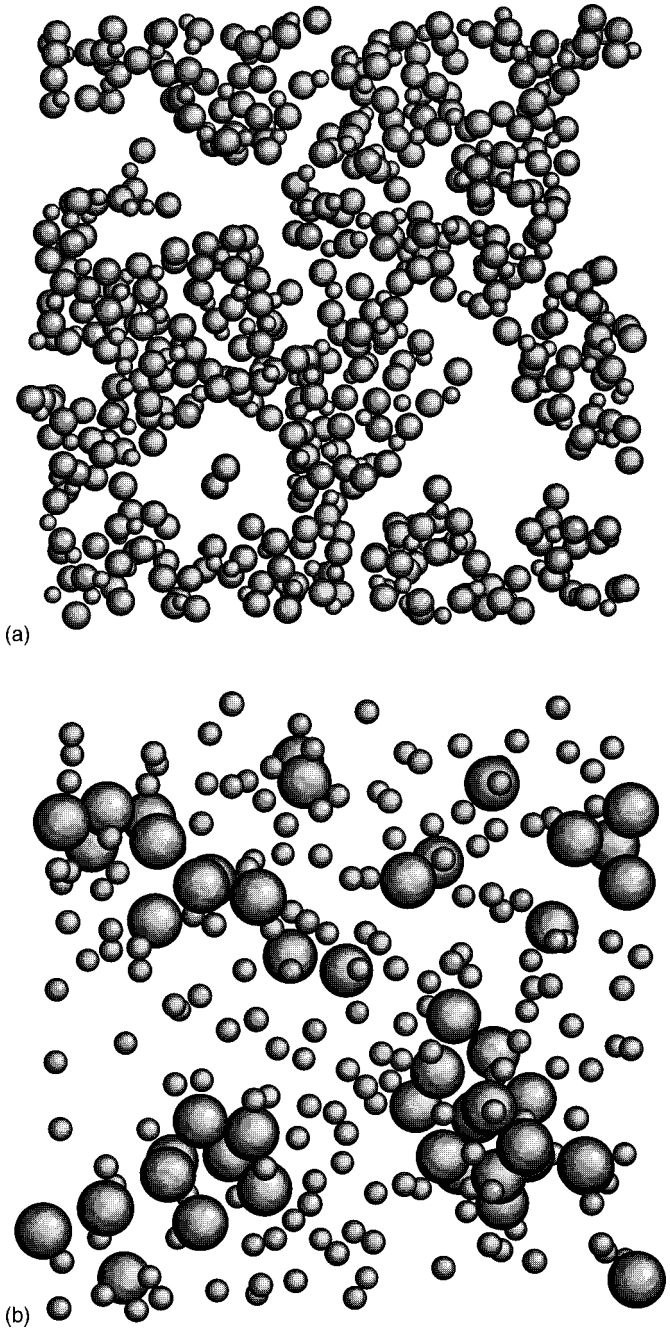

FIG. 10. A 10-Å-thick slice of the RMC configuration of LiCl-Li_2O-$2B_2O_3$. (a) shows the structure of the B-O network and (b) the distribution of lithium and chlorine ions. The radii of the chemical components are B=0.5, O=0.8, Li^+=0.7, and Cl^-=1.6 Å.

Figures 9(a) and 9(b) show the structure of the B-O network and the distribution of lithium ions, respectively, in the undoped glass, and Figs. 10(a) and 10(b) show the B-O structure and the distribution of Li^+ and Cl^- ions, respectively, for the doped glass. The figures show a 10-Å-thick slice of the two RMC configurations. By comparing figures 9(a) and 10(a) the dopant-salt-induced expansion of the B-O network is clearly visible. The voids in the B-O network of the doped glass [see Fig. 10(a)] are, as the partial structure factors indicated, of widely different sizes and geometrical shapes. Both the lithium ions of the undoped glass [see Fig. 9(b)] and the lithium and chlorine ions of the doped glass [see Fig. 10(b)] seem to be randomly distributed in the available voids of the B-O network. Some smaller clusters of LiCl can be observed in the largest voids of the B-O network [see Fig. 10(b)]. The structural pictures of the sodium borate glasses are very similar to the corresponding pictures of the lithium borate glasses, and will, therefore, not be shown here.

2. Short-range order

Figures 11(a) and 11(b) show the partial pair-correlation functions $G_{ij}(r)$ for Li_2O-$2B_2O_3$ and Na_2O-$2B_2O_3$, respectively. The partial pair-correlation functions involving corre-

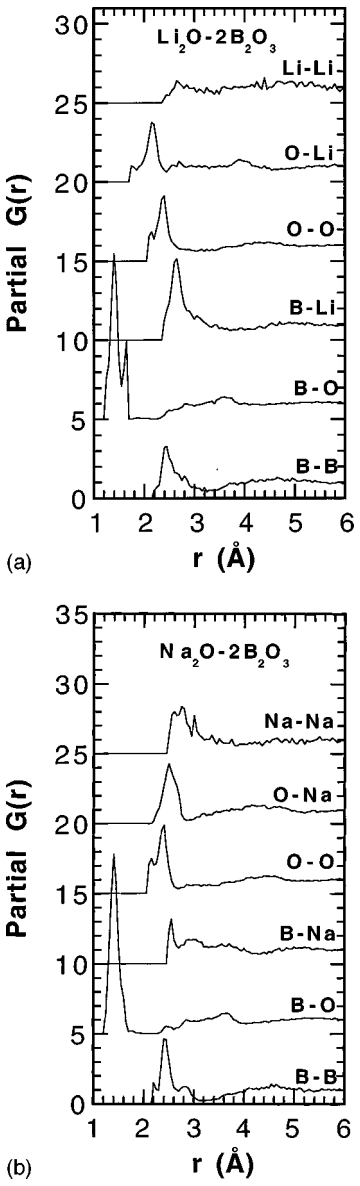

FIG. 11. Partial pair-correlation functions $G_{ij}(r)$ calculated from the RMC configurations of (a) Li_2O-$2B_2O_3$ and (b) Na_2O-$2B_2O_3$. The upper curves have been shifted vertically for clarity.

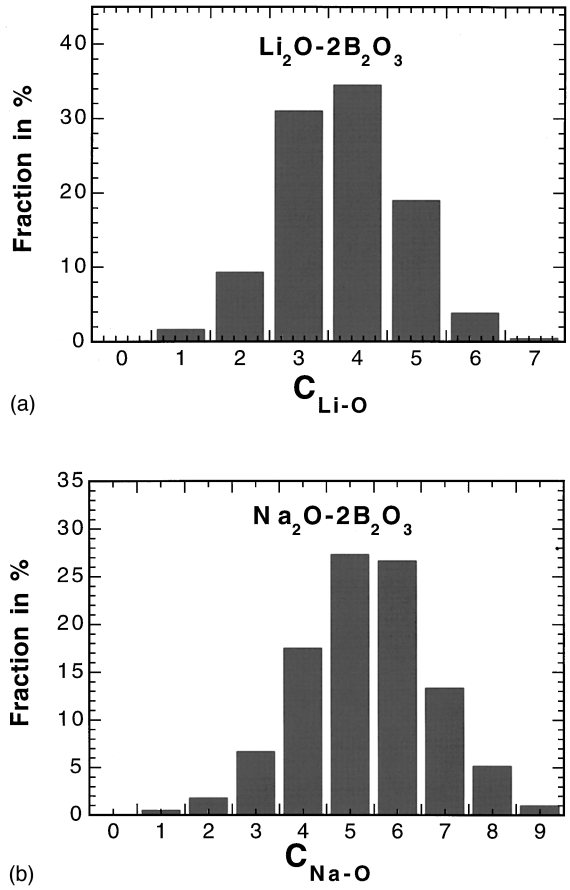

FIG. 12. Distributions of M-O coordination numbers calculated from the RMC configurations of (a) Li_2O-$2B_2O_3$ and (b) Na_2O-$2B_2O_3$.

lations within the B-O network, i.e., $G_{BB}(r)$, $G_{BO}(r)$, and $G_{OO}(r)$, are very similar for the two glasses. The only significant differences are observed in the other three partials with the alkali ions involved. The first peak in $G_{NaO}(r)$ is located at a higher r value (2.45 Å) than in $G_{LiO}(r)$ (2.15 Å) and the M-B distance seems to be more well defined in the lithium borate glass, while the M-M distance is most well defined in Na_2O-$2B_2O_3$. The larger M-O distance in the sodium borate glass is in agreement with experimental findings[33,38,39] and it is, of course, due to the larger size of the Na^+ ion compared to the Li^+ ion. The differences in size and M-O coordination number (see below) between the sodium and lithium ions may explain the differences in $G_{MB}(r)$ and $G_{MM}(r)$, although it should be noted that we are not sure about the validity of details on this level. Such details may not be completely correct in a RMC-produced structural model simply due to the fact that the experimental diffraction data contain a limited amount of structural information. Furthermore, one should note that the nearest Na-Na and Li-Li distances are both about 2.8 Å, which is significantly shorter than in the corresponding crystalline compounds.[35,36,40]

The distributions of M-O coordination numbers are shown in Figs. 12(a) and 12(b) for Li_2O-$2B_2O_3$ and Na_2O-$2B_2O_3$, respectively. It is evident from the figures that the distributions are very wide (perhaps too wide in these RMC models due to the limited information content of the diffraction data and the fact that the RMC method tends to produce the most disordered structure) and that many different coordinations exist. The results suggest that the alkali ions are relatively randomly located in the voids of the B-O network, without having any well-defined local environments or affecting the nearest B-O structures significantly. The average coordination numbers of the nearest Li-O ($r < 2.4$ Å) and N-O ($r < 3.0$ Å) distances are estimated to be about 3.7 and 5.4, respectively. Both values are in agreement (within the experimental errors) with values obtained from direct estimations of neutron[33] and x-ray[38] diffraction data.

The partial pair-correlation functions of LiCl-Li_2O-$2B_2O_3$ and NaCl-Na_2O-$2B_2O_3$ are shown in Figs. 13(a) and 13(b), respectively. The figures show that the first peaks in $G_{ij}(r)$, not involving Cl correlations, are similar to the corresponding peaks of the undoped glasses and that the differences between the two undoped glasses are maintained in the

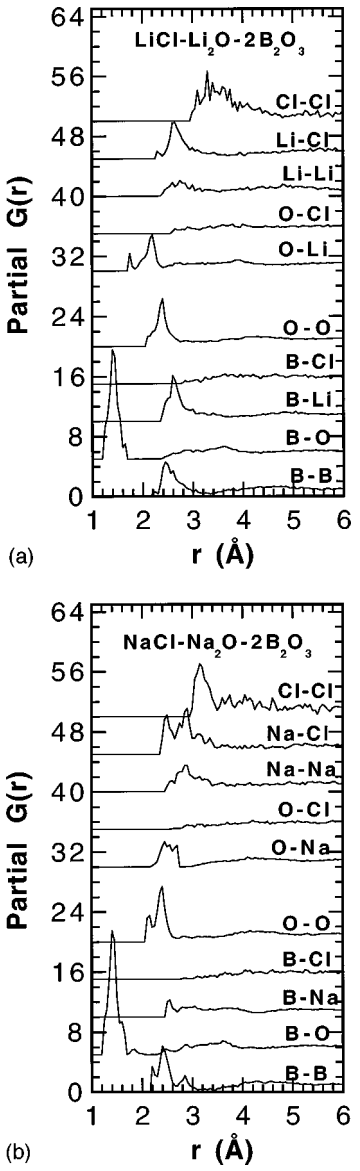

FIG. 13. Partial pair-correlation functions $G_{ij}(r)$ calculated from the RMC configurations of (a) LiCl-Li_2O-$2B_2O_3$ and (b) NaCl-Na_2O-$2B_2O_3$. The upper curves have been shifted vertically for clarity.

doped glasses. The partials $G_{\mathrm{BCl}}(r)$ and $G_{\mathrm{OCl}}(r)$ show no pronounced peaks, which indicates that the chlorine ions are very weakly connected to the B-O network in these glasses. The first Cl-Cl peak is broad and no second M-Cl peak is observed, indicating that no larger MCl clusters are present and that any local ''saltlike structures'' of the present glasses are very disordered.

The disordered nature of the salt ion distributions is also supported in Figs. 14(a) and 14(b), which show the distributions of M-O and M-Cl coordination numbers for LiCl-Li_2O-$2B_2O_3$ and NaCl-Na_2O-$2B_2O_3$, respectively. The figures show that most of the M^+ ions are coordinated to both oxygens and chlorine ions and that many different combinations of coordinations are likely to exist, although one again can suspect that the coordination distributions in the model configurations may be too disordered. The average Li-Cl and Na-Cl coordination numbers ($r<3.2$ Å) are estimated to 1.3 and 1.5, respectively, and the average Li-O and

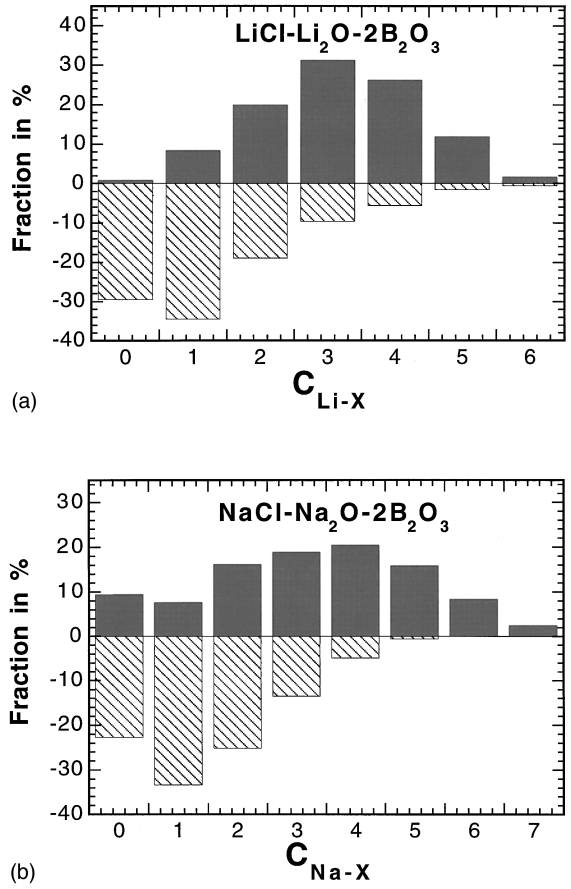

FIG. 14. Distributions of M-O (positive bars) and M-Cl (negative bars) coordination numbers calculated from the RMC configurations of (a) LiCl-Li_2O-$2B_2O_3$ and (b) NaCl-Na_2O-$2B_2O_3$.

Na-O coordination numbers are lower for the doped glasses (3.1 and 3.3, respectively) than for the corresponding undoped glasses. Unfortunately, we have not been able to find any direct experimental determinations of these coordination numbers for the present glasses to compare with, but it is interesting to note that the average Li-O and Na-O coordination numbers are significantly higher than for the corresponding AgI-doped borate glass.[25,57] The reason for this will be discussed in the next section.

V. DISCUSSION

The model of Krogh-Moe for the structure of borate glasses[58] suggests that the glass structure is locally built up by the same structural units as in the corresponding crystal. The model has been supported by many investigations,[49–53,59] which have shown that the arrangement of the network-modifier atoms in metal oxide modified glasses are very similar to that of the related crystals. Since the short-range order of the boron-oxygen network seems to be almost unchanged by the introduction of the metal-halide salt we suggest that also the metal-halide-doped borate glasses investigated here are built up by similar borate units as in the crystalline counterparts.

In the previous section we found that the reason for the decreased correlation length (in the sense that the FSDP moves to higher Q) in the LiCl-doped glass is that there is no

particular intermediate range characteristic distance. Rather there are voids within the B-O network of a wide variety of sizes [see Fig. 10(a)], which would then not give rise to any particular low-Q feature in the structure factor. The structural picture is different from that of the corresponding AgI-doped borate glass,[25] for which AgI doping results in a significant ordering between neighboring network segments with a characteristic length of about 8 Å. This is consistent with the experimental observation for the AgI-doped glasses of a new intense sharp diffraction peak appearing at about 0.8 $Å^{-1}$. From structural pictures it was easy to recognize a characteristic distance between neighboring ''chains'' of 8 ± 3 Å. The B-O network for the present LiCl-doped glass is much more disordered and it is not possible to identify any typical distance between neighboring borate segments. The large differences in the intermediate structure between the lithium and silver borate glasses are likely to arise from the different ionic-covalent characters of the lithium and silver ions. The Ag^+ ions have a much larger electronegativity and thus a larger tendency to form bonds with significant covalent character than the Li^+ ions. Therefore, it seems that the silver and iodine ions have the ability to cross link between different B-O segments and thereby cause the observed intermediate ordering between neighboring borate chain segments. The cross-linking behavior of the silver and iodine ions is also likely to be the reason for the larger expansion of the B-O network and the significantly lower average M-O coordination number in the AgI-doped glass, compared to the LiCl-doped glass. The larger ionic character of the lithium ions make such cross linking much weaker and less directional, and the intermediate structure of the B-O network will be much less affected than in the case of AgI doping. It is more likely that Li^+ ions just stick into the available voids within the glass network or coordinate to the chlorine ions (if they are present). This also explains the remarkably small differences observed in the low-Q range of the structure factor when B_2O_3 is network modified with Li_2O. The structural pictures of the lithium borate glasses are also in agreement with a structural model in which the glass network is built up by a disordered mixture of different kinds of borate configurations (diborate, tetraborate, metaborate, etc.) of different sizes. The introduction of a dopant salt will tend to decrease the density of the glass network and make the overall packing of these borate configurations less dense. The created voids will, as mentioned above, have a large range of sizes and they will be partly filled with lithium and chlorine ions.

A similar structural model for the Na-borate glasses seems to be in rather good agreement with the experimental findings if one takes the short-range differences between the lithium and sodium borate glasses into consideration. Since the cations predominantly bridge between oxygens of different BO_4^- groups[33,60] and the M-O distance is larger for Na^+ than for Li^+,[33] the Na-borate glasses should have lower number densities and longer length scales of the density fluctuations than the corresponding Li-borate glasses, provided that the intermediate structural ordering is similar for the two glass systems. The sharpness of the FSDP may seem to be in contradiction to such a loose random-packing model of different borate configurations. However, it may be explained by the fact that the Na_2O-$2B_2O_3$ glass contains only diborate groups, while the Li_2O-$2B_2O_3$ glass consists of the four borate configurations, diborate, tetraborate, metaborate, and loose BO_4^- units, as suggested from ^{10}B NMR results.[49,53] In terms of intermediate-range structure, this is an important difference between the two glasses, because the four borate configurations in Li_2O-$2B_2O_3$ have all very different shapes and sizes. Hence, the fewer kinds of structural units in the Na-borate glass would cause a more well-defined distance between the structural units and thereby also the observed stronger intermediate-range ordering. The results support the NMR results[49,53] and indicate that the Na-borate glass is slightly more ordered on an intermediate length scale than the Li-borate glass.

When the dopant salts LiCl and NaCl are introduced the FSDP of the B-O network may disappear due to the fact that the dopant ions expand the glass network very inhomogeneously and produce a wide variety of distances between the borate groups, which are likely to be the same as in the corresponding undoped glasses. This is the most probable reason for why no low-Q peak is observed in the neutron diffraction data for LiCl-Li_2O-$2B_2O_3$. A similar phenomenon occurs when NaCl is added to Na_2O-$2B_2O_3$. In this case, the position of the FSDP remains unaffected; however, its intensity decreases dramatically an the RMC-produced structural model indicates that the origin of the peak is completely different for the doped glass. The correlations within the B-O network are only giving rise to a very weak peak at about 1.2 $Å^{-1}$ and an increasing intensity towards $Q=0$, which is the reason for the experimentally observed broadening of the low-Q side of the FSDP.

Next, we turn to the implications of the present structural findings for the possible relation between structure and conductivity. Since the local-structural arrangements of the investigated glasses are very similar to the corresponding crystalline structures,[35,36,40] and these crystals have negligible ionic conductivities, we suggest that the much higher conductivities of the glasses are not due to any specific local-structural arrangement. Rather, the intermediate-range disorder and the lower average number density leads to a more open structure (at least locally) and the creation of voids and pathways within the structure in which the ionic diffusion can take place. The mobility of the cations will then increase with increasing dopant concentration due to the fact that the added metal-halide salt causes an expansion of the host glass network, which, in turn, facilitates widening of existing doorways and opening of new pathways. There are likely also effects due to a reduced M-O coordination number and thereby a lowering of activation barriers for metal ions close to halide ions. In fact, by combining the present structural findings with previous investigations[24–26] it is evident that the local structure around the cations, the accessible free volume, and the ionic conductivity are all closely linked. It is likely that it is the different ionic-covalent characters of the cations and the different sizes and polarizabilities of the salt ions that determine the coordinations of the cations. These local differences induce structural differences also on an intermediate length scale, which, in turn, affect the accessible free volume. As an example, we can take the comparably low average Ag-O coordination numbers and large intermediate-range ordering within the BO and PO network of the AgI-doped borate[25] and phosphate glasses,[24] which are

likely caused by the large electronegativity of the Ag^+ ion. These structural features give rise to a larger accessible free volume for the cations, and thereby also a higher ionic conductivity, than in the more disordered LiCl- and NaCl-doped borate glasses, which also have higher average M-O coordination numbers. Thus, although the accessible free volume is determined by the microscopic interactions we recognize that Tuller and Button's[61] general idea that an open glass structure is essential for high ionic conductivity seems to hold for the present glasses as well as for most salt-doped oxide glasses.[62] Finally, we note that the experimental results show no evidence of any metal-halide clusters of significant size. Hence, the present results imply that structural models for ion conduction based on relatively large salt clusters (>10 Å) (Refs. 16–22) can immediately be rejected for these glasses, as well as for the AgI-doped borate, phosphate, molybdate, and tungstate glasses.[24–26]

VI. CONCLUSION

The following picture of the structures of $(MZ)_x(M_2O\text{-}2B_2O_3)_{1-x}$ ($M=\mathrm{Li,Na}$ and $Z=\mathrm{Cl,Br}$) emerges from using neutron diffraction experiments and reverse Monte Carlo modeling. The dopant metal-halide salt does not affect the short-range order of the B-O network, i.e., the nearest-neighbor distances and the connectivity of the network are preserved. Instead the metal and halide ions enter voids of the structure and simultaneously expand the boron-oxygen network. There does not appear to exist any particular intermediate range ordering in the glasses, apart from that given by packing and requirements to keep the connectivity of the network. This is then in contrast to earlier findings for silver-halide-doped borate glasses.[25] However, the sodium borate glasses appear to be slightly more ordered on an intermediate length scale than the corresponding lithium glasses. This may be an effect of that the network of the Na-diborate glass is built up almost entirely by diborate groups, whereas in the Li-diborate glass many different kinds of borate groups of different shapes and sizes are present.

The short-range order of all the glasses appears to be very similar to that of the corresponding crystalline compounds. Thus, we find no particular short-range ordering that can explain the high ionic conductivity of the glassy state. Rather, we suggest that for the modified but undoped glasses it is the more open and disordered structure that is the main cause of their much higher conductivities than for the crystals. The role of the dopant salt is then, apart from providing more charge carriers and reducing the average M-O coordination number, to further expand the glass network and thereby to promote the formation of open doorways and pathways in the structure suitable for ion conduction.

ACKNOWLEDGMENTS

This work was financially supported by the Swedish Natural Science Research Council. We thank Dr. R. L. McGreevy for providing the RMC code and for helpful discussions.

*Present address: Department of Physics and Astronomy, University College London, London WC1E 6BT, UK.

[1] C. A. Angell, Annu. Rev. Phys. Chem. **43**, 693 (1992).
[2] A. Schiraldi, E. Pezzati, P. Beldani, and S. W. Martin, Solid State Ionics **18/19**, 426 (1986).
[3] C. Chiodelli, A. Magistris, M. Villa, and J. L. Bjorkstam, J. Non-Cryst. Solids **51**, 143 (1982).
[4] G. Carini, M. Cutroni, A. Fontana, G. Mariotto, and F. Rocca, Phys. Rev. B **29**, 3567 (1984).
[5] L. Börjesson, L. M. Torell, and W. S. Howells, Philos. Mag. B **59**, 105 (1989).
[6] L. Börjesson, L. M. Torell, U. Dahlborg, and W. S. Howells, Phys. Rev. B **39**, 3404 (1989).
[7] D. Ravaine and J. L. Souquet, Phys. Chem. Glasses **18**, 27 (1977).
[8] D. Ravaine and J. L. Souquet, Phys. Chem. Glasses **19**, 115 (1978).
[9] D. Ravaine, J. Non-Cryst. Solids **73**, 287 (1985).
[10] A. M. Glass and K. Nassau, J. Appl. Phys. **51**, 3756 (1980).
[11] P. Maass, A. Bunde, and M. D. Ingram, Phys. Rev. Lett. **68**, 3064 (1992).
[12] A. Bunde, M. D. Ingram, P. Maass, and K. L. Ngai, J. Non-Cryst. Solids **131-133**, 1109 (1991).
[13] A. Bunde, M. D. Ingram, and P. Maass, J. Non. Cryst. Solids **172-174**, 1222 1222 (1994).
[14] T. Minami, J. Non-Cryst. Solids **73**, 273 (1985).
[15] G. N. Greaves, J. Non-Cryst. Solids **71**, 203 (1985).
[16] M. Tachez, R. Mercier, J. P. Malugani, and A. J. Dianoux, Solid State Ionics **18-19**, 372 (1986).
[17] M. Tachez, R. Mercier, J. P. Malugani, and A. J. Dianoux, Solid State Ionics **20**, 93 (1986).
[18] J. P. Malugani, M. Tachez, R. Mercier, A. J. Dianoux, and P. Chieux, Solid State Ionics **23**, 189 (1987).
[19] A. Fontana, F. Rocca, and M. P. Fontana, Phys. Rev. Lett. **58**, 503 (1987).
[20] A. Fontana, F. Rocca, and M. P. Fontana, Philos. Mag. B **56**, 251 (1987).
[21] C. Rousselot, M. Tachez, J. P. Malugani, R. Mercier, and P. Chieux, Solid State Ionics **44**, 151 (1991).
[22] C. Rousselot, J. P. Malugani, R. Mercier, M. Tachez, P. Chieux, A. J. Pappin, and M. D. Ingram, Solid State Ionics **78**, 211 (1995).
[23] M. D. Ingram, Philos. Mag. B **60**, 729 (1989); Mater. Chem. Phys. **23**, 51 (1989).
[24] J. Wicks, L. Börjesson, R. L. McGreevy, W. S. Howells, and G. Bushnell-Wye, Phys. Rev. Lett. **74**, 726 (1995).
[25] J. Swenson, L. Börjesson, R. L. McGreevy, and W. S. Howells, Phys. Rev. B **55**, 11236 (1997).
[26] J. Swenson, R. L. McGreevy, L. Börjesson, J. D. Wicks, and W. S. Howells, J. Phys.: Condens. Matter **8**, 3545 (1996).
[27] R. L. McGreevy and L. Pusztai, Mol. Simul. **1**, 359 (1988).
[28] D. A. Keen and R. L. McGreevy, Nature (London) **344**, 423 (1990).
[29] L. Börjesson, Phys. Rev. B **36**, 4600 (1987).
[30] L. Börjesson and L. M. Torell, Solid State Ionics **25**, 85 (1987).
[31] W. S. Howells, Rutherford-Appleton Laboratory, Report No. RAL-80-017, 1980 (unpublished); Rutherford-Appleton Laboratory, Report No. RAL-86-042, 1986 (unpublished).
[32] M. Howe, W. S. Howells, and R. L. McGreevy, J. Phys.: Condens. Matter **1**, 3433 (1989).
[33] J. Swenson, L. Börjesson, and W. S. Howells, Phys. Rev. B **52**, 9310 (1995).

[34] E. Lorch, J. Phys. C **2**, 229 (1969).
[35] J. Kogh-Moe, Acta Crystallogr. **15**, 190 (1962).
[36] J. Kogh-Moe, Acta Crystallogr., Sect. B: Struct. Crystallogr. Cryst. Chem. **24**, 179 (1968).
[37] M. P. Tosi and F. G. Fumi, J. Phys. Chem. Solids **25**, 45 (1964).
[38] G. Paschina, G. Piccaluga, and M. Magini, J. Chem. Phys. **81**, 6201 (1984).
[39] M. P. Medda, A. Musinu, G. Piccaluga, and G. Pinna, J. Non-Cryst. Solids **162**, 128 (1993).
[40] J. Kogh-Moe, Acta Crystallogr., Sect. B: Struct. Crystallogr. Cryst. Chem. **30**, 578 (1974).
[41] C. Kittel, *Introduction to Solid State Physics*, 6th ed. (Wiley, New York, 1986).
[42] M. C. Abramo, G. Pizzimenti, and A. Consola, Philos. Mag. B **64**, 495 (1991).
[43] N. Metropolis, A. W. Rosenbluth, M. N. Rosenbluth, A. H. Teller, and E. Teller, J. Phys. Chem. **21**, 1087 (1953).
[44] R. L. McGreevy, Annu. Rev. Mater. Sci. **22**, 217 (1992).
[45] R. L. McGreevy, Nucl. Instrum. Methods Phys. Res. A **354**, 1 (1995).
[46] D. A. Keen, Phase Transit. **61**, 109 (1997).
[47] G. E. Jellison, Jr., S. A. Feller, and P. J. Bray, Phys. Chem. Glasses **19**, 52 (1978).
[48] Y. H. Yun and P. J. Bray, J. Non-Cryst. Solids **27**, 363 (1978).
[49] S. A. Feller, W. J. Dell, and P. J. Bray, J. Non-Cryst. Solids **51**, 21 (1982).
[50] F. Galeener, G. Lucovsky, and J. C. Mikkelsen, Jr., Phys. Rev. B **22**, 3983 (1980).
[51] J. Lorösch, M. Couzi, J. Pelous, R. Vacher, and A. Levasseur, J. Non-Cryst. Solids **69**, 1 (1984).
[52] E. I. Kamitsos, A. P. Patsis, M. A. Karakassides, and G. D. Chryssikos, J. Non-Cryst. Solids **126**, 52 (1990).
[53] G. E. Jellison, Jr. and P. J. Bray, J. Non-Cryst. Solids **29**, 187 (1978).
[54] S. R. Elliott, Phys. Rev. Lett. **67**, 711 (1991).
[55] S. R. Elliott, J. Phys.: Condens. Matter **4**, 7661 (1992).
[56] J. H. Lee and S. R. Elliott, Phys. Rev. B **50**, 5981 (1994).
[57] G. Licheri, A. Musinu, G. Pashina, G. Piccaluga, G. Pinna, and A. Magistris, J. Chem. Phys. **85**, 500 (1986).
[58] J. Krogh-Moe, Phys. Chem. Glasses **6**, 46 (1965).
[59] P. H. Gaskell, J. Zhao, P. Boden, and P. Cheuix, J. Non-Cryst. Solids **150**, 80 (1992).
[60] L. Cervinka, F. Rocca, P. Fornasini, and G. Dalba, J. Non-Cryst. Solids **150**, 140 (1992).
[61] H. L. Tuller and D. P. Button, in *Transport-Structure Relations in Fast Ion and Mixed Conductors*, edited by F. W. Poulsen, N. Hessel-Andersen, K. Clausen, S. Skaarup, and O. Soerensen (Risø National Laboratory, Roskilde, Denmark, 1985), p. 119.
[62] J. Swenson and L. Börjesson, Phys. Rev. Lett. **77**, 3569 (1996).